111-39
24796
P-40

NASA TECHNICAL MEMORANDUM 104079
AVSCOM TR-91-B-005

EFFECT OF INITIAL DELAMINATION ON MODE I AND MODE II INTERLAMINAR FRACTURE TOUGHNESS AND FATIGUE FRACTURE THRESHOLD

Gretchen Bostaph Murri and Roderick H. Martin

May 1991

National Aeronautics and
Space Administration

Langley Research Center
Hampton, Virginia 23665

(NASA-TM-104079) EFFECT OF INITIAL DELAMINATION ON MODE 1 AND MODE 2 INTERLAMINAR FRACTURE TOUGHNESS AND FATIGUE FRACTURE THRESHOLD (NASA) 40 p CSCL 20K

N91-26569

G3/39 Unclas 0024796

SUMMARY

Static and fatigue double-cantilever beam (DCB) and end-notch flexure (ENF) tests were conducted to determine the effect of the simulated initial delamination on interlaminar fracture toughness, G_c, and fatigue fracture threshold, G_{th}. Unidirectional, 24-ply specimens of S2/SP250 glass/epoxy were tested with Kapton inserts at the midplane at one end, to simulate an initial delamination. Four insert thicknesses were used - 13, 25, 75, and 130 μm. Some specimens were also tested with either tension or shear precracks as the initial delamination. To determine G_{th}, fatigue tests were conducted by cyclically loading specimens until delamination growth was detected. The fatigue fracture threshold was defined to be the maximum cyclic strain energy release rate, G_{max}, below which no delamination growth would occur in less than $1x10^6$ cycles.

For the DCB specimens, consistent values of mode I fracture toughness, G_{Ic}, were measured for specimens with inserts of thickness 75 μm or thinner, or with shear precracks. The fatigue DCB tests gave similar values of G_{Ith} for the 13, 25, and 75μm specimens. Results for the shear precracked specimens were significantly lower than for specimens without precracks.

Results for both the static and fatigue ENF tests showed that measured G_{IIc} and G_{IIth} values decreased with decreasing insert thickness, so that no limiting thickness could be determined. Results for specimens with inserts of 75 μm or thicker were significantly higher than the results for precracked specimens or specimens with the 13 or 25 μm inserts.

Keywords: delamination, ENF, DCB, strain energy release rate, fracture toughness, mode I, mode II, fatigue, fatigue fracture threshold

Nomenclature

A	constant in delamination growth law
a	delamination length
a_0	initial delamination length
B	exponent in delamination growth law
b	specimen width
C	specimen compliance, δ/P
$\frac{da}{dN}$	delamination growth per loading cycle
E_{11}	axial modulus of specimen
G	strain energy release rate
G_I	mode I strain energy release rate
G_{II}	mode II strain energy release rate
G_c	interlaminar fracture toughness
G_{Ic}	mode I interlaminar fracture toughness
G_{IIc}	mode II interlaminar fracture toughness
G_{max}	maximum cyclic strain energy release rate
G_{Imax}	maximum cyclic strain energy release rate for mode I loading
G_{IImax}	maximum cyclic strain energy release rate for mode II loading
G_{th}	fatigue fracture threshold for delamination growth onset
G_{Ith}	mode I fatigue fracture threshold
G_{IIth}	mode II fatigue fracture threshold
G_{13}	transverse shear modulus for a unidirectional laminate
h	specimen half-thickness
L	ENF specimen half-span
m	constant for DCB compliance expression

n	exponent for DCB compliance expression
P	out-of-plane load
P_c	maximum load in static ENF test
P_{max}	maximum load in cyclic DCB test
P_{NL}	load at which load-displacement curve becomes nonlinear
R	$\delta_{min}/\delta_{max}$ in fatigue tests
δ	load-point displacement
δ_{max}	maximum load-point displacement under cyclic loading
δ_{min}	minimum load-point displacement under cyclic loading

Introduction

In order to optimize the use of fiber-reinforced composite materials in primary aircraft structures, the damage tolerance of such materials under both static and fatigue loading must be established. The most common failure mechanism in laminated composites is delamination. Therefore, characterization of a composite material must include measurement of its interlaminar fracture toughness. However, there are still important unresolved issues concerning the measurement of interlaminar fracture toughness. The opening (mode I) and sliding shear (mode II) fracture toughnesses can be measured as a delamination grows in a specimen with a simulated initial delamination. This study considered the effect of several different types of initial delamination on interlaminar fracture toughness measured using the double-cantilever beam (DCB) and end-notched flexure (ENF) specimens under static and fatigue loading.

The DCB and ENF specimens are typically used to measure the delamination strain energy release rates due to mode I (tension) and mode II (shear) loading, respectively. Both of these tests may be performed statically to determine interlaminar fracture toughness, G_c, or cyclically to determine a fatigue fracture threshold, G_{th}, below which no delamination growth will occur. The DCB and ENF specimens are unidirectional laminates with an insert at the midplane at one end to simulate an initial delamination. During the manufacture of the specimen, a resin pocket may form at the tip of the insert. The size of the resin pocket depends on the thickness of the insert. A delamination starting at the insert tip must first extend beyond this resin pocket before it can grow along the interface between two plies. Values of G_c and G_{th} measured for a delamination growing through the resin pocket may be unconservative [1,2].

One method that has been used to avoid the problem of propagating the delamination through the resin pocket is to precrack the specimen. That is, before testing, the initial delamination is extended through the resin pocket and a short distance along the midplane, creating a sharp delamination front.

A mode I, or tension, precrack may be created by wedging open the delamination faces until a delamination grows through the resin pocket. The disadvantage of this method is that it can cause fiber bridging. In the DCB specimen, fiber bridging increases the apparent opening mode strain energy release rate, G_I, as the delamination continues to grow [3-6]. However, in structural configurations, delamination usually occurs between plies of different orientation where fiber bridging would not be present. Therefore, only the values of G_I measured before fiber bridging begins can be considered a material property. Reference 7 indicated that tension precracking may be unsuitable for the ENF specimen as well. If fiber bridging exists in the ENF specimen after tension precracking, the bridged fibers must be broken before the delamination can grow under the shear loading. This may result in higher values of G_{II} than if no fiber bridging was present.

Alternatively, a shear precrack may be created by using the ENF test fixture to apply a shear load to either the DCB or ENF specimen. The shear precracking does not cause fiber bridging, but it may create damage ahead of the delamination tip [8] that would not be present in a delamination not formed in shear, nor in a structure in which delaminations initiate at a structural discontinuity. This damage may result in measuring overly conservative values of G.

For composite materials under fatigue loading, the problems of fiber bridging and damage ahead of the delamination front must also be considered.

Fatigue crack growth in metals has typically been characterized by relating crack growth per loading cycle to a cyclic stress intensity factor [9]. For composites, this method was modified to relate delamination growth to cyclic strain energy release rate using a power law of the form $da/dN=AG_{max}^{B}$, where da/dN is the delamination growth rate per fatigue cycle. The constants A and B are determined experimentally [10-12]. However, refs. 10-12 showed that for both the DCB and ENF specimens, the exponent B is so large (as high as 10 for the DCB specimen) that small errors in the applied load can result in large errors (up to an order of magnitude) in the predicted delamination growth rate. For example, for the DCB specimen with a material for which B=9, a 10% error in the applied load value reduces the predicted da/dN by 61%. Therefore, the delamination growth approach is not suitable as a damage tolerance analysis for composites.

An alternative method for determining a fatigue fracture threshold for fatigue loading was proposed in ref. 12 and demonstrated for AS4/PEEK material. Each test specimen was cyclically loaded until delamination growth could be detected in the specimen. Specimens were tested over a range of G_{max} values, and the log of the number of cycles to delamination growth onset (log N) was plotted against G_{max}. Specimens that reached approximately 1 to 3 million cycles without delaminating were considered runouts. In this way a fatigue fracture threshold, G_{th}, below which delamination will not occur at less than 1 million cycles can be determined. However, the specimens used in ref. 12 contained inserts of 130μm thickness, and it is not certain how these thick inserts may have affected the results.

In this study the effects of the insert thickness and precracking techniques on G_c and G_{th} are investigated for both DCB and ENF specimens. The DCB test results are from ref. 5. Tests were conducted on glass/epoxy

specimens with Kapton inserts of either 13, 25, 75, or 130 μm thickness, without precracks, growing the delamination directly from the insert tip. Tests were also conducted on specimens with precracks as the initial delamination. For the DCB specimens, shear precracks were created in specimens with 13μm inserts. For the ENF specimens, both tension and shear precracks were grown from various thickness inserts. Results are compared for each type of initial delamination, for both specimens.

Materials

Schematic diagrams of the DCB and ENF specimens are shown in figs. 1 and 2, respectively. The specimens used in this study were 24-ply unidirectional specimens of S2/SP250 glass/epoxy made from a 122°C cure prepreg manufactured by 3M Corp. Panels were laid up at the NASA Langley Research Center, using four different thicknesses of Kapton film - 13, 25, 75, and 130 μm - for the inserts. To prevent the inserts from adhering to the laminate surfaces, the insert material was sprayed with a release agent before the panels were cured. In this study, calculations were performed assuming material properties of E_{11}=45.5 GPa, and G_{13}=6.07 GPa.

The DCB and ENF specimens were cut from the same panels. All specimens were approximately 25 mm wide and had a nominal thickness, 2h, of 4.7 mm. The DCB and ENF specimens were approximately 146 and 159 mm long, respectively, with inserts approximately 57 mm long. The specimens were determined to have an average fiber volume fraction of 62.8%.

Load was applied to the DCB specimens through piano hinges, indicated in fig. 1, which were bonded to the specimen with Hysol EA9309, a two-part, room-temperature cure adhesive. Prior to testing, the DCB and ENF specimens were dried for 19 hours. The drying process consisted of heating for 1 hour at 95°C, 1 hour at 110°C, 16 hours at 125°C, and 1 hour at 150°C. After the

specimens cooled to room temperature they were stored in a dessicator until tested.

Experimental Procedure

Double Cantilevered Beam

The DCB test apparatus is shown in fig. 3. Static DCB tests were conducted under displacement control, at a cross-head displacement rate of 0.5 mm/min. The beam-opening displacement, δ, was measured using the displacement of the cross-head. Load was applied to the specimen until the delamination had extended approximately 12mm from the insert tip. An X-Y chart recorder was used to record the load and displacement of the specimen.

The fatigue DCB tests were also run under displacement control, in a servo-hydraulic loading machine, using an R-ratio of 0.5, and a frequency of 10 Hz. Delamination growth onset was determined by monitoring the specimen edge with an optical microscope of 60X magnification and recording the number of loading cycles at delamination growth onset. Testing was continued until the delamination had grown approximately 0.25 mm. To obtain a curve relating the maximum cyclic G at delamination growth onset, G_{Imax}, and the corresponding number of loading cycles to delamination growth onset, N, specimens with different insert thicknesses or with shear precracks were cycled, using a range of different maximum displacements.

End-Notched Flexure

The ENF test fixture, shown in fig. 4, was mounted in a servo-hydraulic load frame. The specimen rested on the two outer rollers and load was applied by the center roller. These rollers were mounted on ball bearings and were free to rotate. Because the specimen was delaminated on only one end, it deflected unsymmetrically, resulting in small side forces which tended to shift the specimen on the rollers as load was applied. The

restraining bar shown in fig. 4 prevented shifting of the specimen and was free to rotate as the specimen deflected during the test. The total span between the outer rollers, 2L, was 101.6 mm. The specimen was placed on the rollers so that the distance from the outer roller to the tip of the insert, a_0, was approximately L/2 (fig. 2). The specimen displacement was measured by means of a direct-current differential transducer (DCDT) mounted under the center of the specimen, with the rod supported by a spring. Prior to loading, the location of the outer load point was marked on the specimen, for use later in determining the initial delamination length. Tests were conducted both statically and in fatigue, under displacement control. To determine G_{IIc}, specimens were loaded at a cross-head displacement rate of 2.5 mm/min until they delaminated. The load and center point displacement were recorded with an X-Y chart recorder. The specimens failed unstably in every case, with the delamination extending rapidly from the insert to the point under the central roller or slightly past it.

Cyclic ENF tests were run using the same apparatus as the static ENF tests. Specimens were loaded to the mean load and were then cycled sinusoidally at a frequency of 10 Hz and an R-ratio of 0.5. Each specimen was cycled until delamination growth onset could be detected. By testing at a range of cyclic G_{IImax} values, a threshold was determined below which delamination growth would not occur. An optical microscope with magnification of 32X was mounted to the test stand to aid in visually determining the onset of delamination growth. Additionally, delamination growth was detected using the load output of the test stand load cell. Under displacement control, as the delamination grows, the maximum load decreases. Therefore, the load output was monitored with a digital voltmeter. Delamination growth of about 0.2 mm corresponded to an approximate 2% drop in the indicated load value. If a specimen reached

approximately 1 million to 3 million loading cycles with no indication of delamination growth onset, it was considered a runout and the test was stopped.

Pre-cracking

Specimens of both the DCB and ENF laminates were tested with precracks. Both tension and shear loading were used to precrack the ENF specimens; only shear precracks were used for the DCB specimens because tension precracks initiate fiber bridging which increases the initial G_{Ic} value and the results are therefore meaningless. Shear precracks were created for both the DCB and ENF specimens using the ENF test fixture. Specimens were positioned in the fixture so that the initial delamination length was slightly less than the half-span, L. The specimen was then loaded statically to delamination growth onset. The delamination extended to a point just under the central loading roller. For the ENF specimens, an optical microscope with magnification of 32X was used to locate the tip of the new delamination front, which was then marked on the specimen edge. After testing, the laminate was completely split by hand along the midplane to expose the fracture surfaces, and the exact location of the delamination tip prior to testing was determined by observing the delaminated surfaces. The previously mentioned load point mark was then used to determine the actual value of initial delamination length, a_0, to use in data reduction. If the precracking had not produced a straight delamination front, a_0 was determined to be the average of the initial delamination lengths at the edges and in the center of the specimen.

Tension precracks were created in the ENF specimens by clamping the specimens across the width, just ahead of the insert tip, and inserting a thin wedge (such as a putty knife blade) at the insert end of the laminate. The surfaces were pried apart until the delamination grew to the clamp. The

new delamination front was located using the same technique that was used for the shear precracked specimens. In ref. 8, it was shown that surfaces that delaminated under tension loading look markedly different from surfaces that delaminated due to shear. Also, surfaces that delaminated under the same type of loading have a different appearance depending on whether the load was applied statically or cyclically. Therefore, for all cases except the ENF specimens with shear precracks that were tested statically, it was easy to verify the assumed delamination tip location in the precracked specimens after testing, by splitting the specimen and examining the delamination surfaces. The method of locating the new delamination tip with a microscope after precracking proved to be very accurate for the cases that could be checked after testing and therefore was assumed to be equally good for the static ENF tests with shear pre-cracks.

Data Reduction

The equations used in this study to calculate the various strain energy release rates are given in the following section. They are based on classical linear beam theory expressions. Further explanation and derivations can be found in ref. 13 and 14 for the DCB and ENF tests, respectively.

Double Cantilever Beam

The static fracture toughness, G_{Ic}, was calculated using eq. (1),

$$G_{Ic} = \frac{n P \delta}{2 b a} \tag{1}$$

where n, the exponent in the equation relating specimen compliance to delamination length ($\delta/P=ma^n$), was determined by testing, and ranged between 2.37 and 2.56, with an average value of 2.52. The effect of fiber bridging on the value of n was not taken into account. As fiber bridging occurs, the measured compliance decreases and hence values of n will decrease.

Because the effect on n is difficult to quantify, however, the experimentally determined value of n was used. This was considered a conservative approach.

The visually observed onset of delamination growth from an insert corresponded to a deviation from linearity in the load-displacement plot, as shown in fig. 5. The loads and displacements corresponding to this deviation from linearity were used in eq.(1). However, for the specimens that were precracked in shear, the P-δ curve prior to delamination growth onset was non-linear, as in fig. 6, possibly indicating a change in the shape of the damage zone. Because there is no well-defined linear region for those cases, G_{Ic} was determined using the load and displacement values corresponding to delamination growth visible at the edges. The maximum mode I strain energy release rate for cyclic loading was calculated from eq. (2), using the average value of n (n=2.52) from the static tests, and the maximum cyclic load and displacement at the first cycle.

$$G_{Imax} = \frac{n\, P_{max}\, \delta_{max}}{2\, b\, a} \tag{2}$$

End-Notched Flexure

In ref. 8 it was shown that the beam theory equation for G_{IIc} with a correction for transverse shear agreed very well with predicted values from a 2D finite element analysis for specimens with delamination lengths in the range used in this study. This equation is of the form

$$G_{II} = \frac{9P^2a^2C}{2b(2L^3+3a^3)}\left[1 + 0.2(E_{11}/G_{13})(h/a)^2\right] \tag{3}$$

where C is the compliance of the ENF specimen and the E_{11}/G_{13} term in eq.(3) is the shear correction term. A typical ENF load-displacement diagram for a specimen with a shear precrack is shown in fig. 7. For the shear precracked and 13 and 25 μm insert specimens, the curve was relatively linear from the

beginning of loading until the specimen was close to the final failure load. Just before the specimen delaminated unstably, the P-δ curve became nonlinear. The final failure load and the load at the deviation from linearity are indicated on the figure as P_c and P_{NL}, respectively. A greater degree of load-displacement nonlinearity was evident for the specimens with inserts thicker than 25μm, and in specimens with tension precracks. The onset of nonlinearity in the curve may be an indication of the beginning of subcritical delamination growth in the laminate. However, the delamination growth occurred very rapidly and no visual observation of the beginning of delamination growth was possible. Therefore, mode II fracture toughness values were calculated using both P_c and P_{NL} for the value P in eq.(3). The compliance, C, was the slope of the initial linear portion of the curve for both calculations.

Results and Discussion

Resin Pockets

Figures 8-10 show photos of the region around the insert tip for specimens with 13, 25, and 130 μm inserts, respectively. There is no obvious resin pocket for the 13 μm insert. However, a resin pocket is visible at the tip of the 25 μm insert, and there is a very obvious resin pocket associated with the 130 μm inserts.

Static Tests

Figure 11 shows G_{Ic} results for the DCB tests. As the delamination was allowed to grow in the static tests, fiber bridging was evident and resulted in a large (factor of 6) increase in G_{Ic}. Therefore, the values of G_{Ic} in fig. 11 represent the initial delamination growth; that is, before any fiber bridging. The values shown are averages, with the number of specimens of each type tested indicated on the figure, along with the range of the data.

The most scatter was observed for the 130μm insert specimens, where the measured G_{Ic} values were within ±10% of the mean value. The measured fracture toughnesses are very similar for specimens with insert thicknesses of 13, 25, and 75 μm and for those with shear precracks. These results are consistent with the results of ref. 15 on adhesive bond thickness effects of an epoxy resin on mode I fracture toughness. Reference 15 showed that an increase in fracture toughness occurred for bond thicknesses greater than 63.5 μm for a toughened epoxy resin (BP907).

Figure 12 shows the results for G_{IIc}, calculated using P_c and P_{NL}. For each case, the bars represent the average value of the listed number of specimens, and the range of the data is indicated. The calculated values for G_{IIc} were within ±13% of the mean values for all except the P_{NL} calculations for the 75μm insert specimens, and both calculations for the shear precracked specimens. Those cases showed significantly more scatter, with the range of the data within ±20% and ±30% of the mean G_{IIc} for the 75μm insert specimens and the shear precracked specimens, respectively. Also, as fig.12 shows, there was more variation in G_{IIc} between the different initial delamination types than there was for the DCB tests. The results calculated using P_c yielded the highest values of G_{IIc} for the two thickest inserts, 75 and 130 μm, and the specimens with 13 and 25 μm inserts yielded the lowest values, with the 13 μm specimens being the lowest of the group. The two types of precracked specimens yielded very similar results that fell between the results for the 25μm and 130μm specimens. In other recent studies, however, the lowest values of G_{IIc} were measured from precracked specimens. For example, ref. 7 shows results for three different composite materials, two with 25μm inserts and one with 13μm inserts. For all three materials the tension precracked specimen resulted in lower values

of G_{IIc} than the specimens tested from the inserts. Also, in ref. 8, shear and tension precracked ENF specimens of T300/BP907 yielded G_{IIc} values that were 25% and 35% lower than values measured from inserts of double layers of 13μm Kapton. The difference in results between refs. 7 and 8 and the current study may be a result of the fact that the glass/epoxy used in this study is very brittle and very prone to fiber bridging.

Results from the same ENF specimens, calculated using P_{NL} in eq. 3, are also shown in fig. 12. In this case the lowest value corresponds to the 130μm inserts, because those specimens exhibited a large amount of nonlinearity in the loading curve, possibly due to plasticity in the large resin pocket. There was also more load-displacement nonlinearity for the tension precracked specimens than for the other types, as shown by the larger differences in G_{IIc} between the P_c and P_{NL} calculations. This may be due to bridged fibers deforming and breaking [7]. The results for the 75 μm inserts, using P_{NL}, were again higher than the other types. The tension precracked specimens and the 13 and 25 μm specimens all had similar G_{IIc} values; the results for the shear precracked specimens were slightly higher. However, excluding the 130μm insert specimens, whether the results are calculated using P_c or P_{NL}, G_{IIc} decreases with decreasing insert thickness without reaching a constant level.

Fatigue Tests

Results of the cyclic DCB tests are shown in fig. 13. Each data point shown represents a single specimen that was cyclically loaded until delamination growth onset was detected, or until it reached between 1 and 3 million cycles with no delamination growth, as indicated by the arrows. The results at $N=10^6$ are similar for the 13, 25 and 75 μm specimens, and the 130μm results are considerably higher. There is considerable scatter in the

data for every specimen type. However, over the full range of N, the results for the specimens with shear precracks are much lower than the results measured from the inserts. The same effect was observed in ref. 12 for a graphite/thermo-plastic composite. The shear precracking process creates damage ahead of the delamination front in the form of micro-cracks [8]. As these micro-cracks coalesce, the delamination grows sooner than it would in an undamaged laminate. Therefore, under fatigue loading, delamination growth onset occurs much sooner in specimens that were precracked in shear.

For each of the specimen types, a visual best-fit curve was drawn as a lower bound to the data set and the fatigue fracture threshold, G_{Ith}, was defined as the value of the curve at $N=1x10^6$ cycles. The various G_{Ith} values are given in fig. 14. The results are consistent with the static results, except for the very low value for the shear precracked case. The G_{Ith} results for the 13, 25, and 75 μm cases are again very similar to each other, whereas values for the 130 μm case are about 40% higher.

Fatigue test results for the ENF specimens are shown in fig. 15. Because the G_{IIc} values for the 75 and 130 μm insert specimens were similar and were much higher than for the thinner inserts, specimens with 130μm inserts were not included in the cyclic tests. Results at $N=1x10^6$ were similar for the two precracked specimen types and the 25 μm insert specimens. Results for the specimens with 75 μm inserts are noticeably higher over the range of N, whereas results for those specimens with 13 μm inserts are considerably lower. Visual best fit curves were drawn through the lower bound of each data set and G_{IIth} values were chosen from the curve at $N=1x10^6$. Those G_{IIth} results are compared in fig. 16. The

results are similar to the static results, in that G_{IIth} decreases with decreasing insert thickness for the three thicknesses tested. The threshold value for the 13 μm insert specimens is much lower than any of the other cases, and is only half the threshold value for the 75 μm insert specimens. The G_{IIth} values for the precracked specimens were in the same range as the results for the 25 μm insert specimens.

Summary of Results

For the glass/epoxy material tested, only the thinnest (13μm) inserts yielded specimens with no visible resin pocket at the insert tip. However, results for the DCB tests under both static and fatigue loading were similar for insert thicknesses up to 75μm. Precracking should not be used for DCB testing, since tension precracks create fiber bridging which results in artificially high values of G_I, and shear precracking creates damage ahead of the delamination front that resulted in very conservative values of G_{Ith}, as well as non-linear load-displacement plots.

For the ENF tests, the thinnest inserts, 13 μm, gave lower G_{IIc} and G_{IIth} values than either the tension or shear precracked specimens. However, the ENF results do not indicate that a limiting value of insert thickness can be chosen. It is possible that a thinner insert material, if available, would result in even lower values of G_{IIc} and G_{IIth}. In similar studies with other composite materials the most conservative (lowest) values of G were measured using precracked specimens. However, in this study of S2/SP250, precracking did not yield the lowest values of G_{IIc} or G_{IIth}. Also, tension precracking caused significant nonlinearity in the P-δ curve, and shear precracking resulted in greater scatter in the data. Until a limiting insert thickness or precracking method can be determined for the

ENF test in general, or for the material being considered, the most conservative approach to measuring mode II strain energy release rates is to use the thinnest insert material available.

Conclusions

Specimens of 24-ply S2/SP250 glass/epoxy material containing midplane inserts to simulate initial delaminations were tested using the DCB and ENF specimens. The specimens were tested statically to determine the interlaminar fracture toughness G_c , and in fatigue to determine the fatigue fracture threshold, G_{th}. To study the effect of the simulated initial delamination on G_c and G_{th}, four different insert thicknesses - 13, 25, 75, and 130 μm - as well as either tension or shear precracks were used. Results of this study showed that for S2/SP250 laminates:

1. A resin pocket will form at the tip of the insert used to simulate the delamination. Thicker inserts will result in thicker resin pockets. However, for the thinnest inserts used in this study (13 μm) no resin pocket was visible.
2. It is best to use the thinnest insert material possible for DCB testing, to eliminate the resin pocket or keep it as small as possible. However, for the material tested in this study, the DCB fracture toughness and fatigue fracture threshold were very similar for insert thicknesses up to 75 μm. Inserts that were 130 μm thick gave significantly higher test results in both cases and should not be used.
3. The static and cyclic ENF tests showed that G_{IIc} and G_{IIth} decrease with decreasing insert thickness, without reaching an apparent limiting level. Therefore, a conservative approach requires that the insert material used for the ENF test should be as thin as possible and not greater than 13μm.

4. Shear precracking creates damage ahead of the delamination front. For the DCB specimens in fatigue, this damage resulted in significantly lower values of fatigue fracture threshold, G_{Ith}.

5. For the ENF specimens, tension and shear precracking yielded similar values of G_{IIc} and G_{IIth}. Results obtained from the precracked ENF specimens were higher than results for the thinnest (13μm) insert specimens.

References

1. Murri, G.B., and O'Brien, T.K.: "Interlaminar G_{IIc} Evaluation of Toughened Resin Matrix Composites Using the End-Notched Flexure Test," AIAA-85-0647, Proceedings of the 26th AIAA/ASME/ASCE/AHS Conference on Structures, Structural Dynamics and Materials, Orlando, FL, April 1985, pp. 197-202.

2. O'Brien, T.K., Johnston, N.J., Raju, I.S., Morris, D.H., and Simonds, R.A.: "Comparisons of Various Configurations of the Edge Delamination Test for Interlaminar Fracture Toughness," Toughened Composites, ASTM STP 937, N.J. Johnston, Ed., American Society for Testing and Materials, Philadelphia, 1987, pp. 275-294.

3. Russell, A.J., "Factors Affecting the Opening Mode Delamination of Graphite/Epoxy Laminates," Defence Research Establishment Pacific (DREP), Canada, Materials Report 82-Q, December 1982.

4. Johnson, W.S., and Mangalgiri, P.D.: "Investigation of Fiber Bridging in Double Cantilever Beam Specimens," Journal of Composites Technology and Research, Vol.9, No.1, Spring 1987, pp.10-13.

5. Martin, R.H.: "Effect of Initial Delamination on G_{Ic} and G_{Ith} Values from Glass/Epoxy Double Cantilever Beam Tests," Proceedings of the American Society for Composites, Third Technical Conference, Seattle, WA, September 1988, pp.688-701.

6. Davies, P., Cantwell, W., and Kausch, H.H.: "Measurement of Initiation Values of G_{Ic} in IM6/PEEK Composites," Composites Science and Technology, Vol. 35, 1989, pp. 301-313.

7. Russell, A.J.: "Initiation of Mode II Delamination in Toughened Composites," Presented at the Third ASTM Symposium on Composite Materials: Fatigue and Fracture, Orlando, FL, November 1989.

8. O'Brien, T.K., Murri, G.B., and Salpekar, S.A.: Interlaminar Shear Fracture Toughness and Fatigue Thresholds for Composite Materials, Composite Materials: Fatigue and Fracture, Second Volume, ASTM STP 1012, Paul A. Lagace, Ed., American Society for Testing and Materials, Philadelphia, 1989, pp. 222-250.

9. Clark, W.G., Jr, and Hudak, S.J., Jr,: "Variability in Fatigue Crack Growth Rate Testing," Journal of Testing and Evaluation, Vol.3, No.6, 1975, pp. 454-476

10. de Charentenay, F.X., Harry, J.M., Prel, Y.J., and Benzeggagh, M.L.: "Characterizing the Effect of Delamination Defect by Mode I Delamination Test," Effect of Defects in Composite Materials, ASTM STP 836, D.J. Wilkins, Ed., American Society for Testing and Materials,Philadelphia, 1984, pp. 84-103.

11. Ramkumar, R.L. , and Whitcomb, J.D.,: "Characterization of Mode I and Mixed Mode Delamination Growth in T300/5208 Graphite/Epoxy," Delamination and Debonding of Materials, ASTM STP 876, W.S. Johnson, Ed., American Society for Testing and Materials, Philadelphia, 1985, pp. 315-335.

12. Martin, R.H., and Murri, G.B.: "Characterization of Mode I and Mode II Delamination Growth and Thresholds in Graphite/PEEK Composites," Composite Materials: Testing and Design, Ninth Volume, ASTM STP 1059, S.P. Garbo, Ed., American Society for Testing and Materials, Philadelphia, 1990, pp. 251-270.

13. Whitney, J.M., Browning, C.E., and Hoogsteden, W., "A Double Cantilever Beam Test for Characterizing Mode I Delamination of Composite Materials," Journal of Reinforced Plastics and Composites, Vol. 1, October 1982, pp. 297-313.

14. Russell, A.J., "On the Measurement of Mode II Interlaminar Fracture Energies," Defence Research Establishment Pacific (DREP), Canada, Materials Report 82-O, December 1982.

15. Chai, H.: "Bond Thickness Effect in Adhesive Joints and its Significance for Mode I Interlaminar Fracture of Composites," Composite Materials: Testing and Design (7th Conference), ASTM STP 893, J.M. Whitney, Ed., American Society for Testing and Materials, Philadelphia, 1986, pp. 209-231.

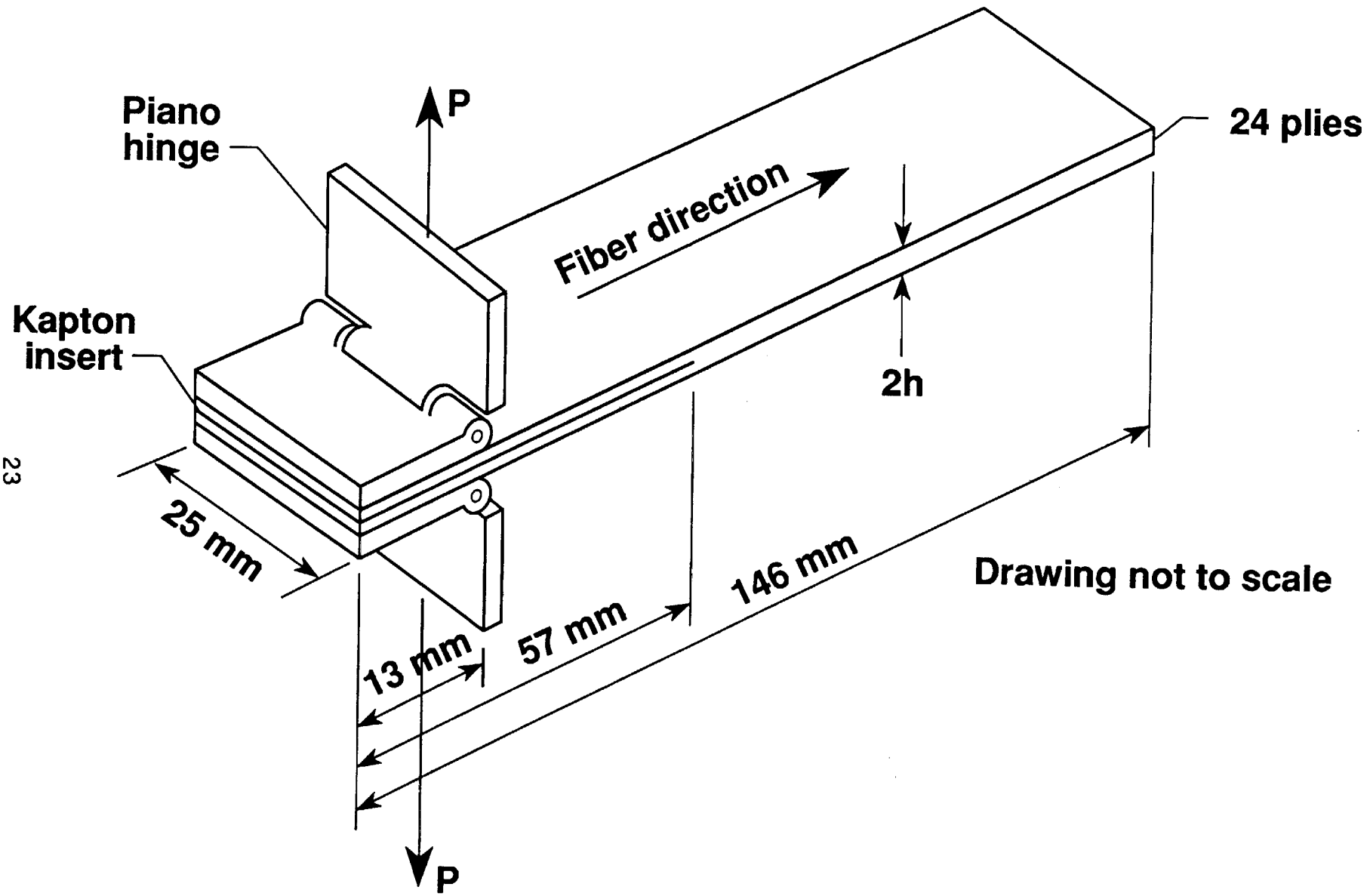

Figure 1. Diagram of DCB specimen.

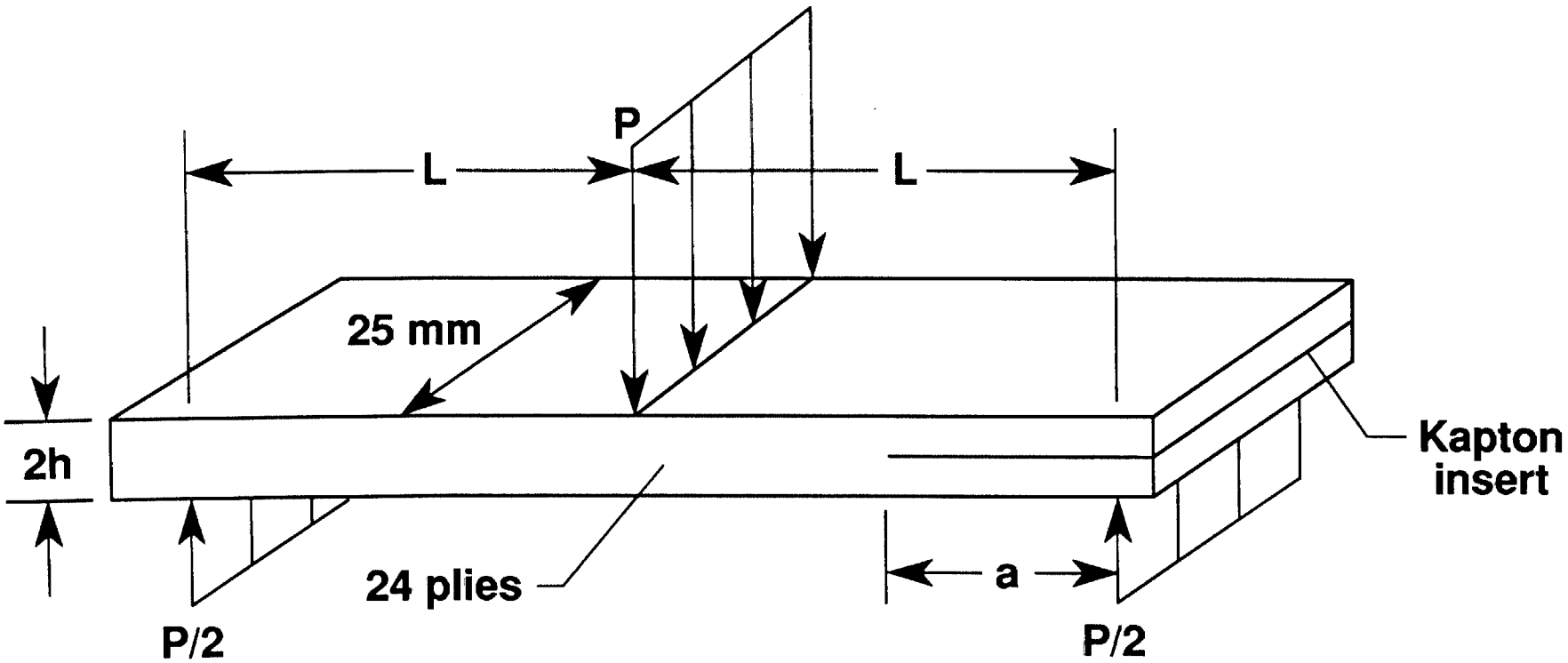

Figure 2. Diagram of ENF specimen.

ORIGINAL PAGE
BLACK AND WHITE PHOTOGRAPH

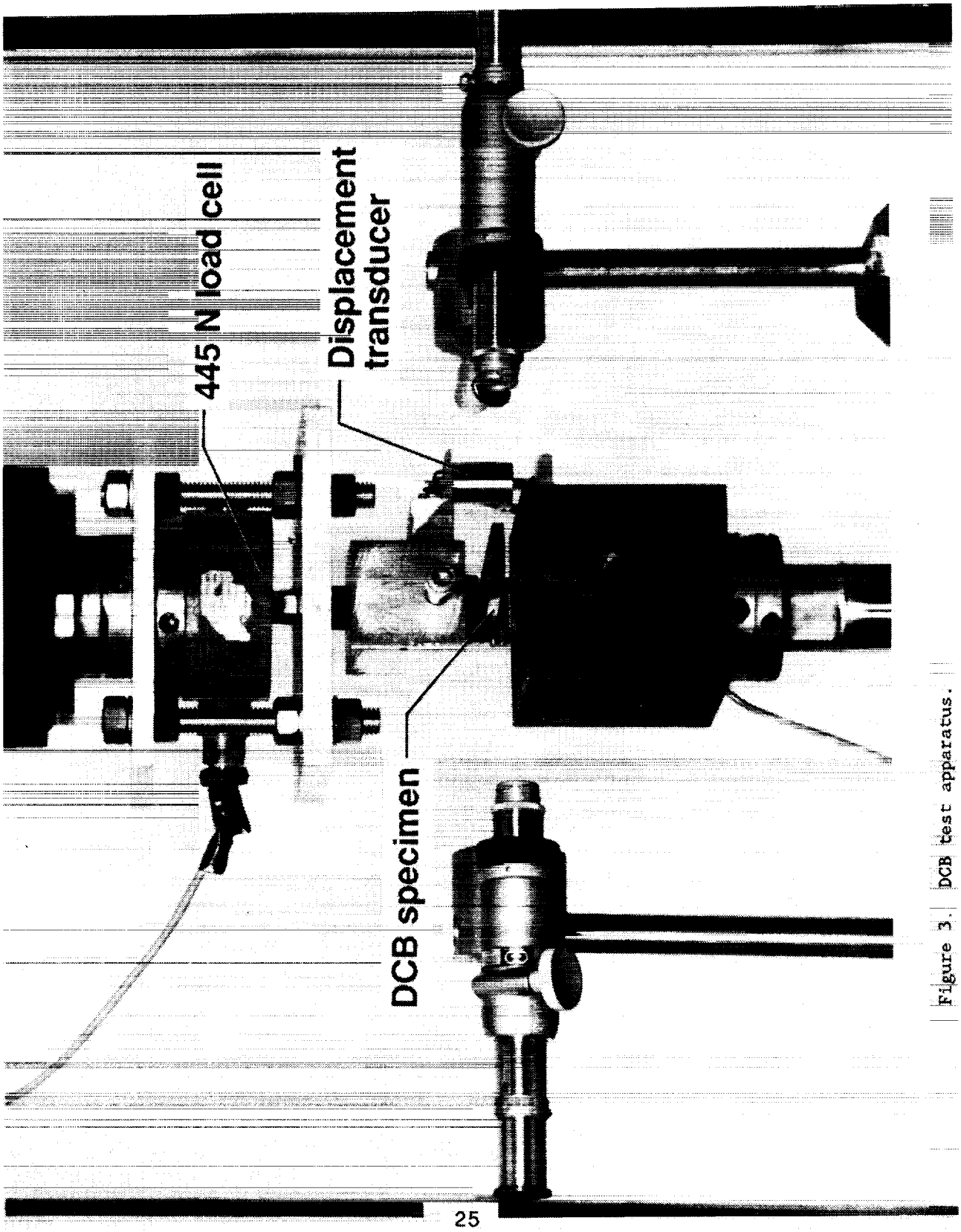

Figure 3. DCB test apparatus.

ORIGINAL PAGE
BLACK AND WHITE PHOTOGRAPH

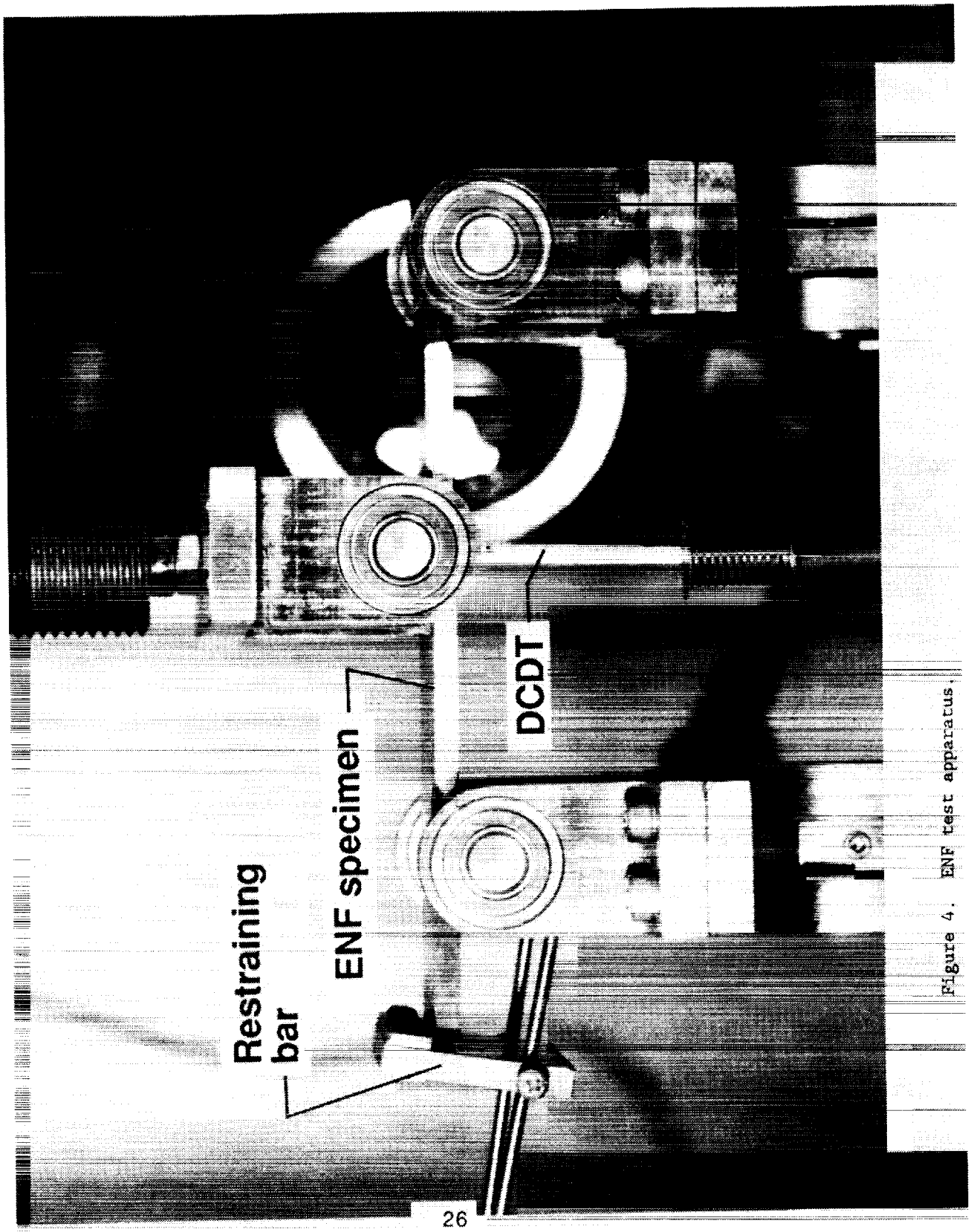

Figure 4. ENF test apparatus.

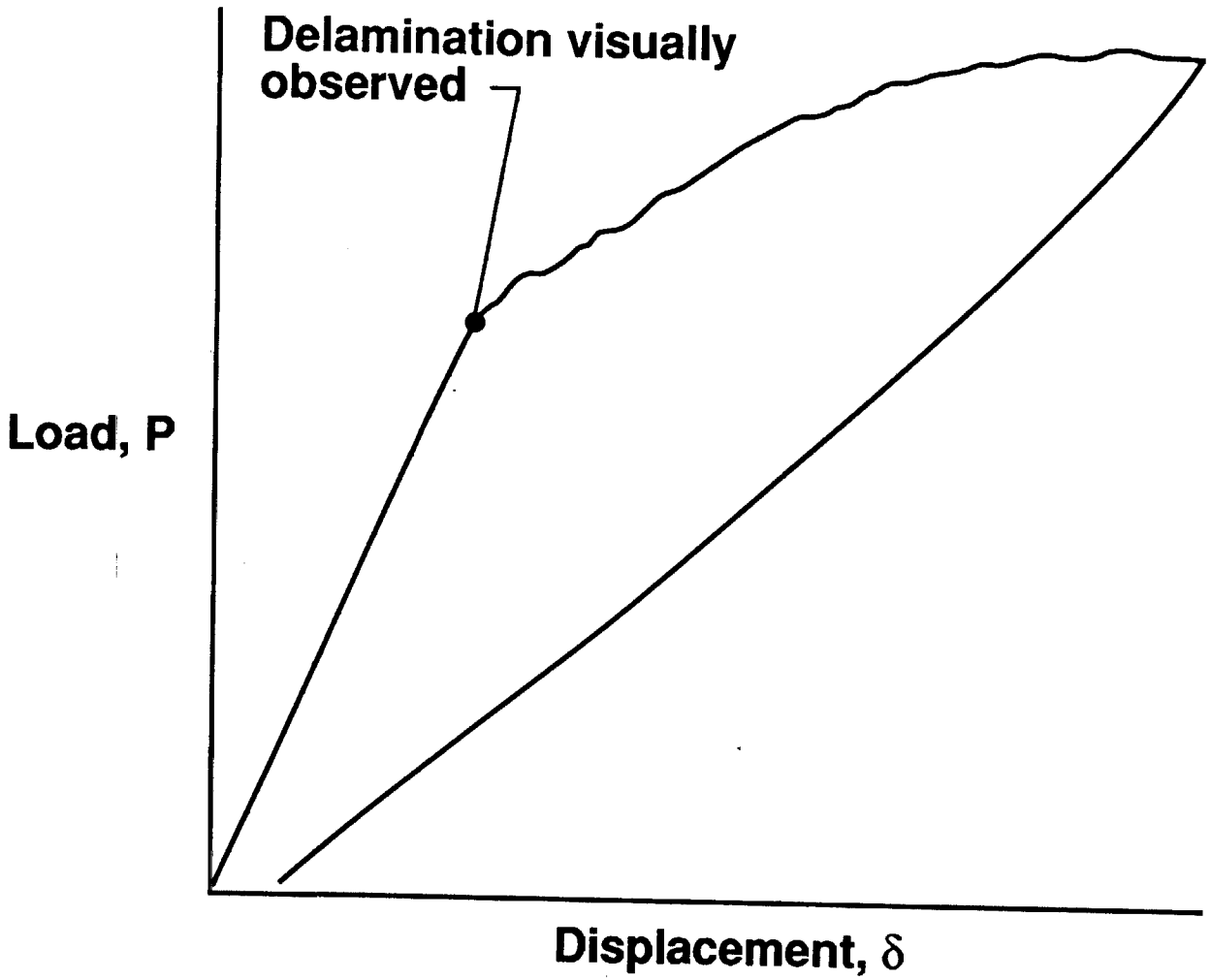

Figure 5. Load-displacement plot for DCB specimen with 13μm insert and no precrack.

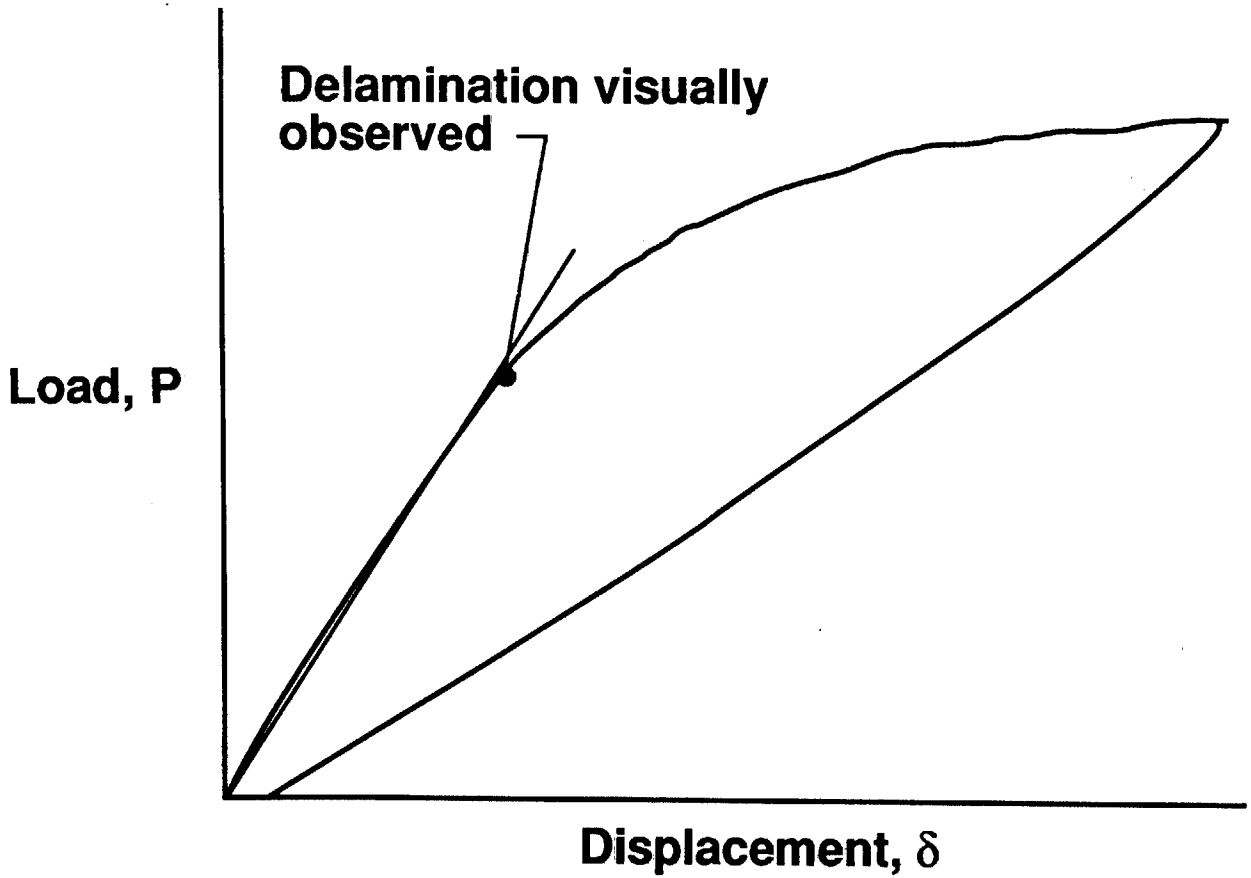

Figure 6. Load-displacement plot for DCB specimen with shear precrack.

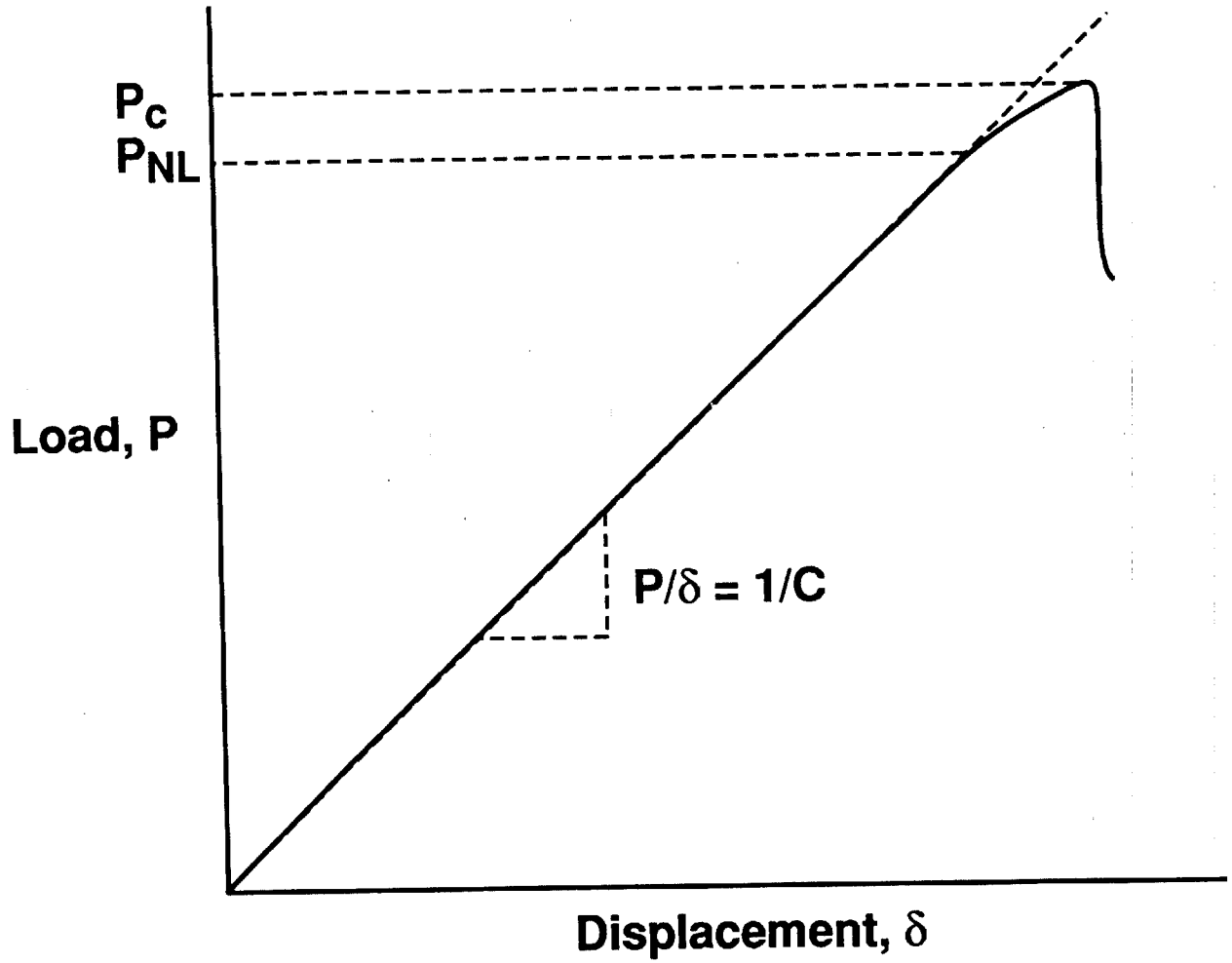

Figure 7. Load-displacement diagram for ENF specimen with shear precrack.

ORIGINAL PAGE
BLACK AND WHITE PHOTOGRAPH

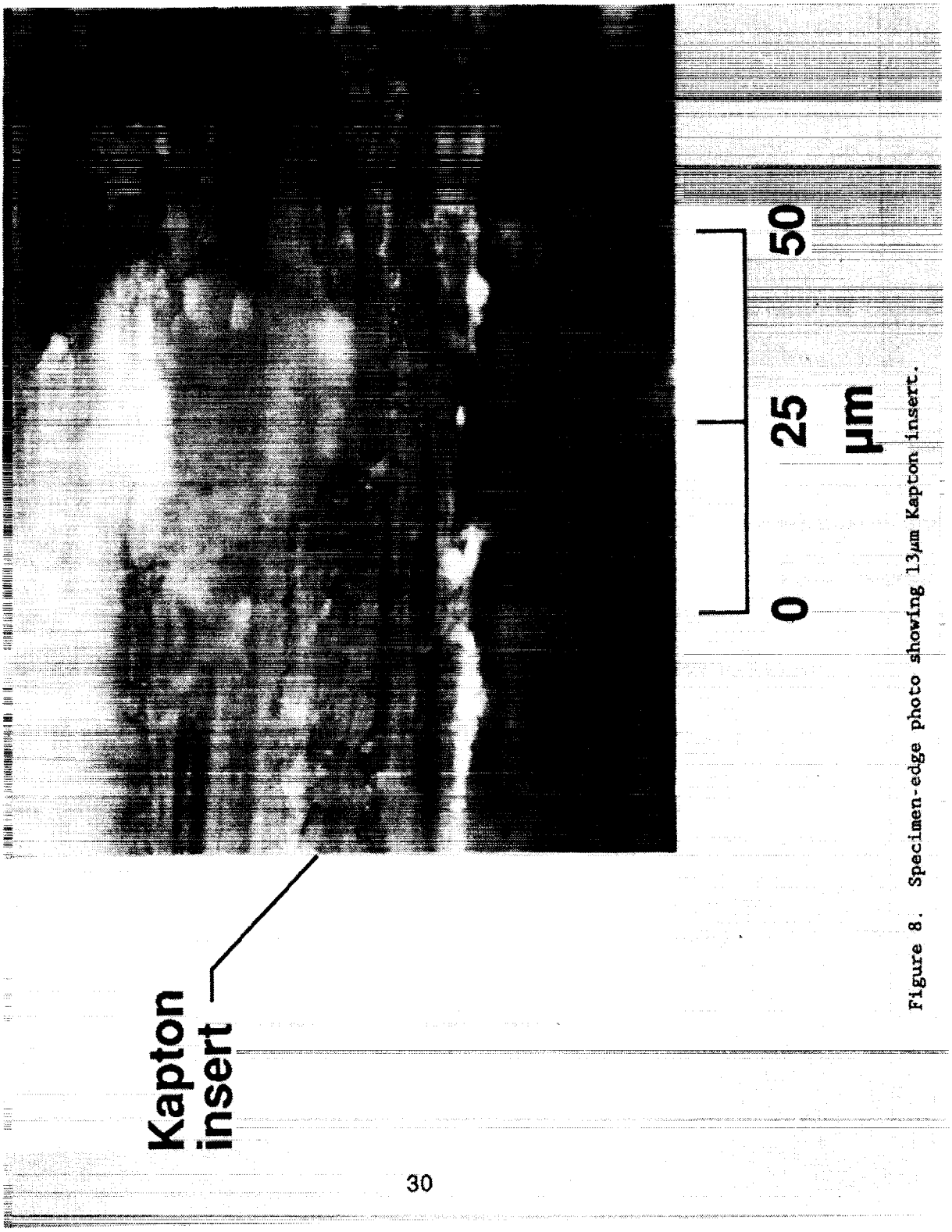

Figure 8. Specimen-edge photo showing 13μm Kapton insert.

ORIGINAL PAGE
BLACK AND WHITE PHOTOGRAPH

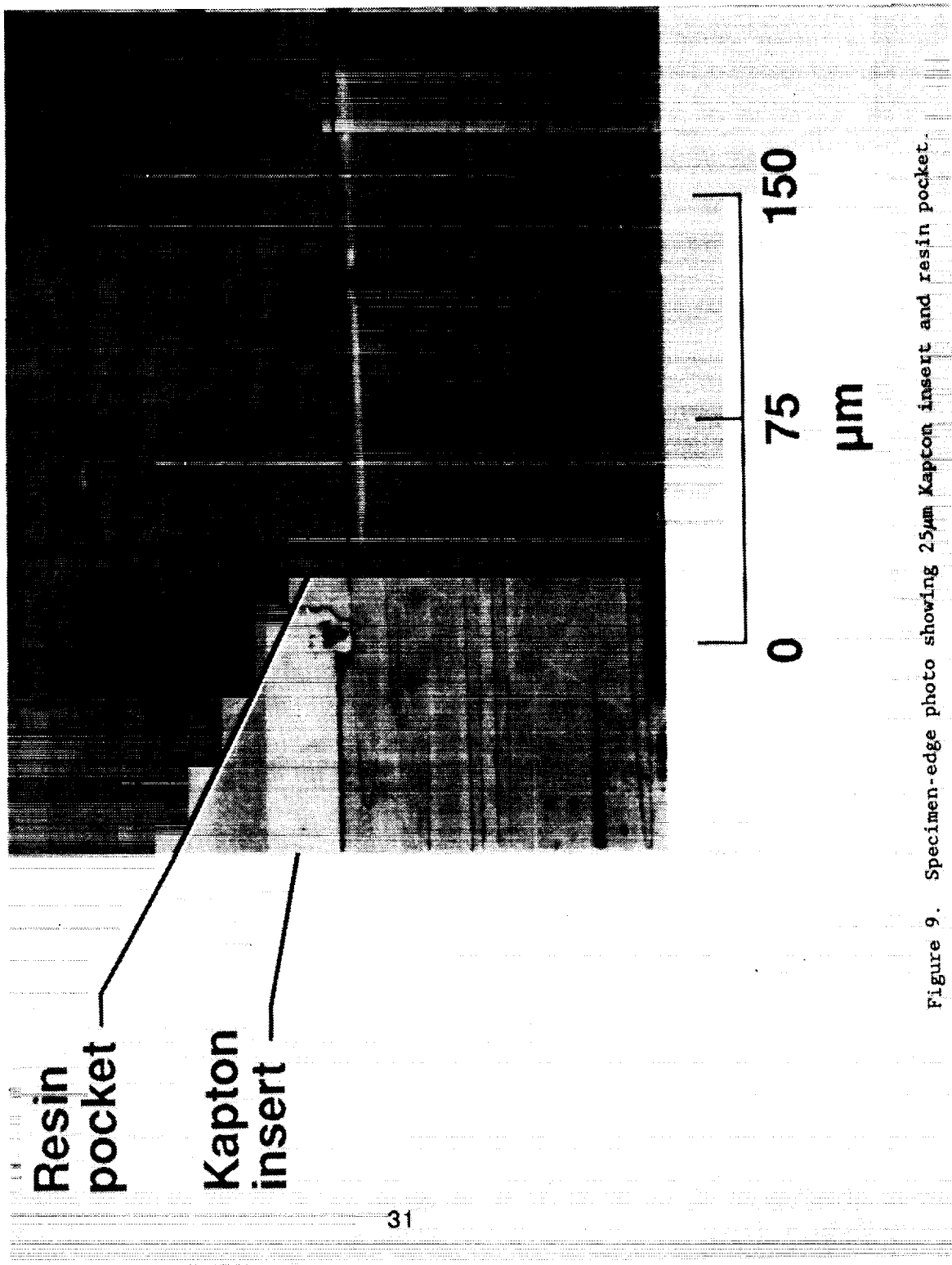

Figure 9. Specimen-edge photo showing 25µm Kapton insert and resin pocket.

ORIGINAL PAGE
BLACK AND WHITE PHOTOGRAPH

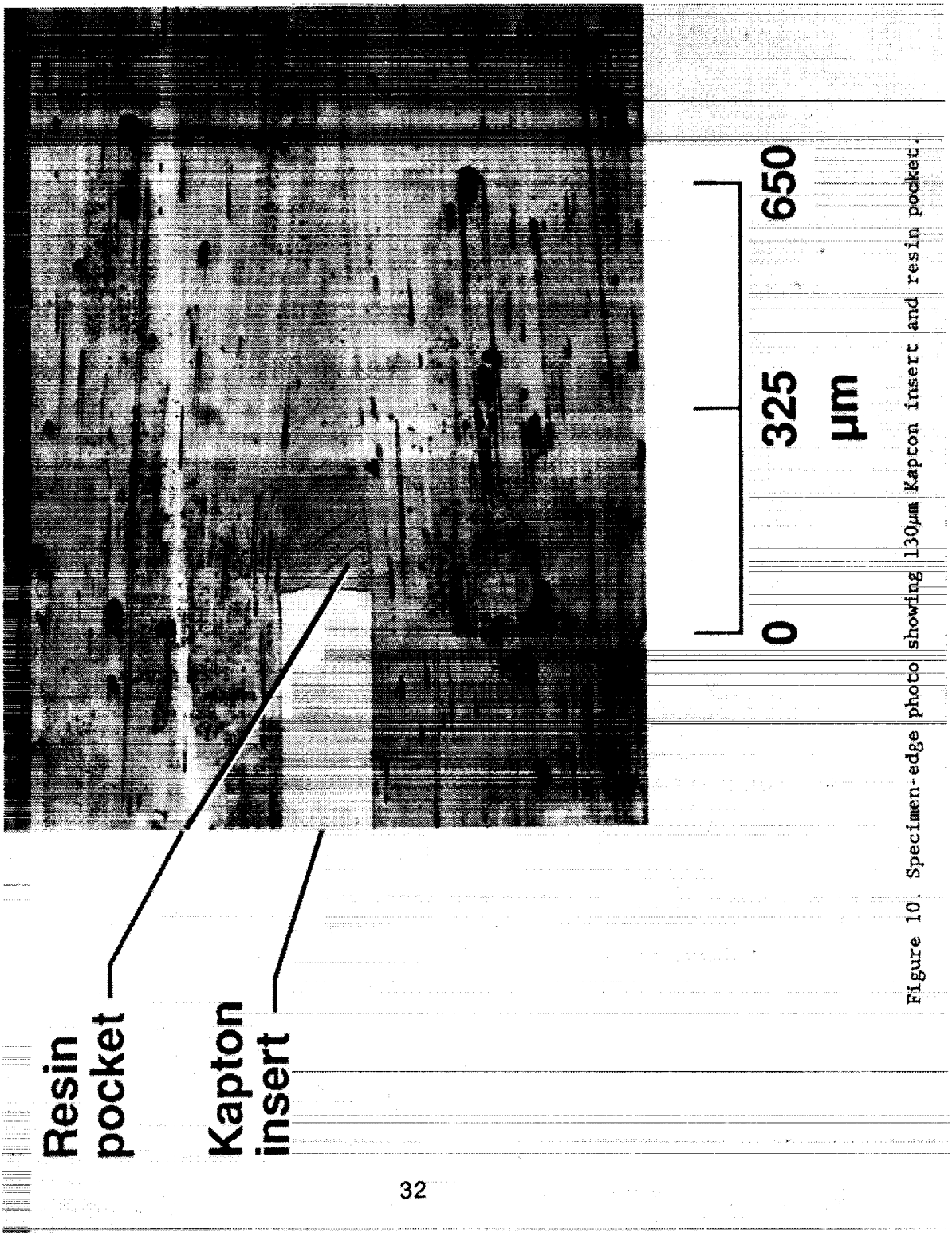

Figure 10. Specimen-edge photo showing 130µm Kapton insert and resin pocket.

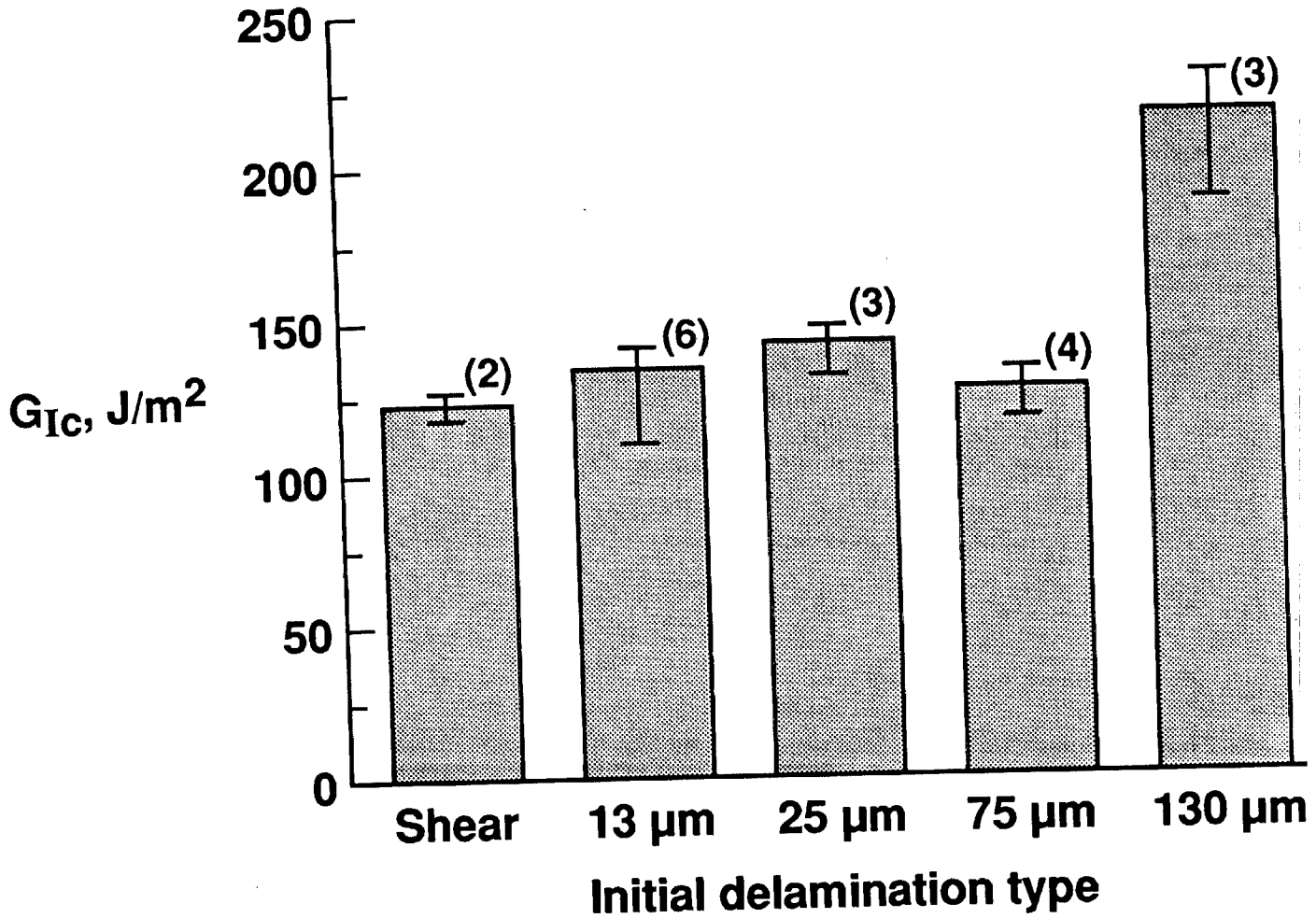

Figure 11. Mode I interlaminar fracture toughness for S2/SP250 DCB specimen.

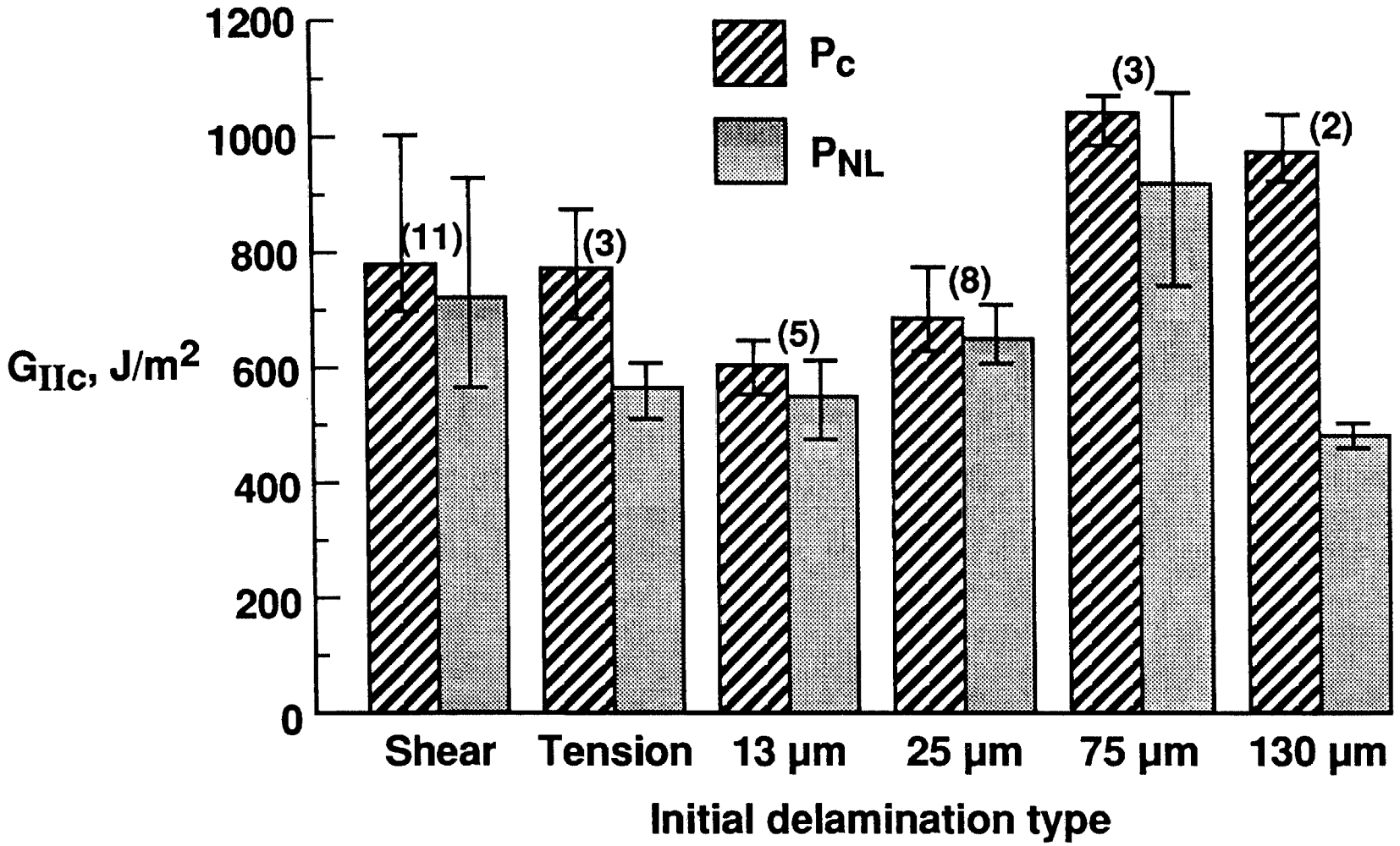

Figure 12. Mode II interlaminar fracture toughness for S2/SP250 ENF specimen.

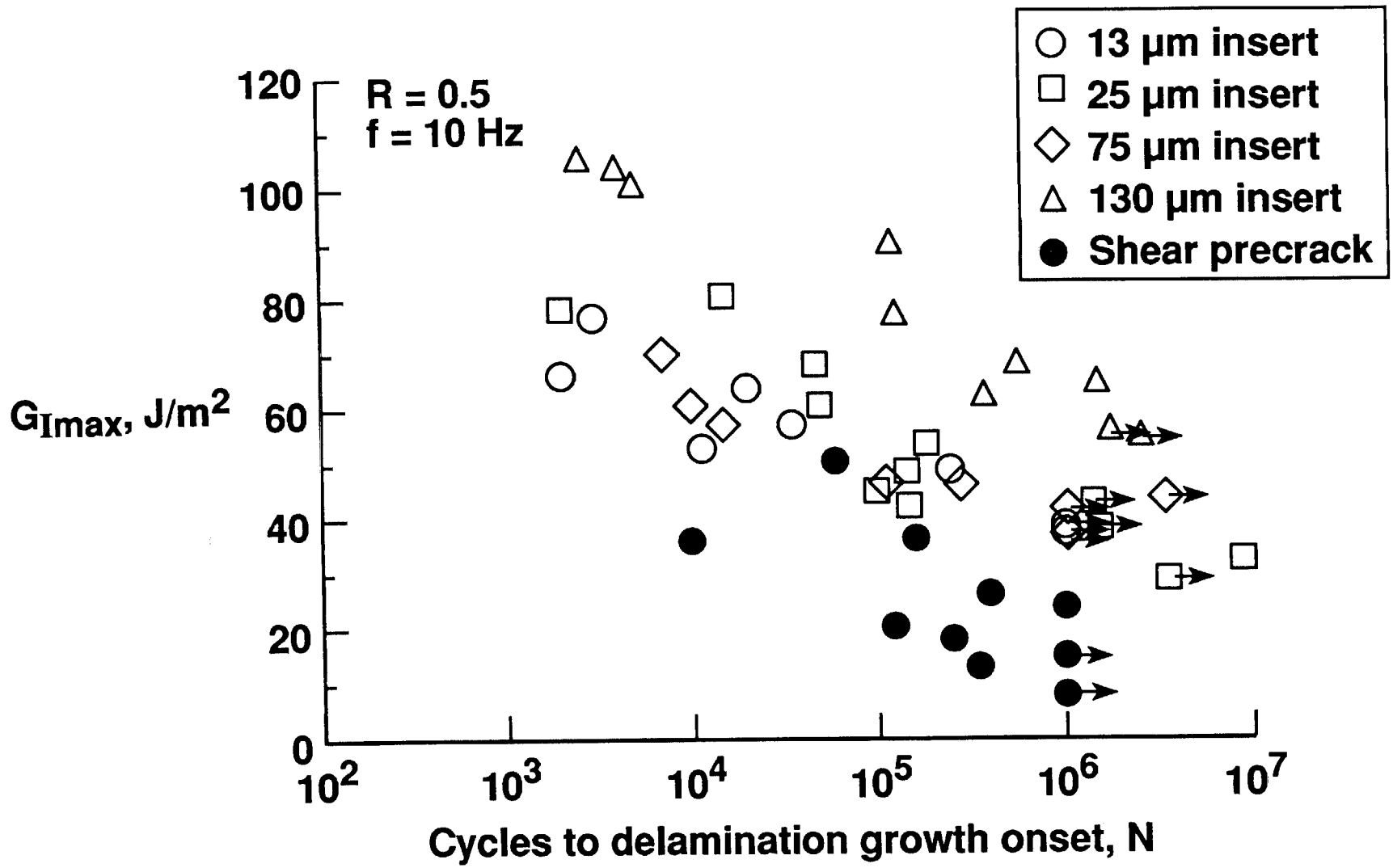

Figure 13. Fatigue delamination growth onset in S2/SP250 DCB specimens.

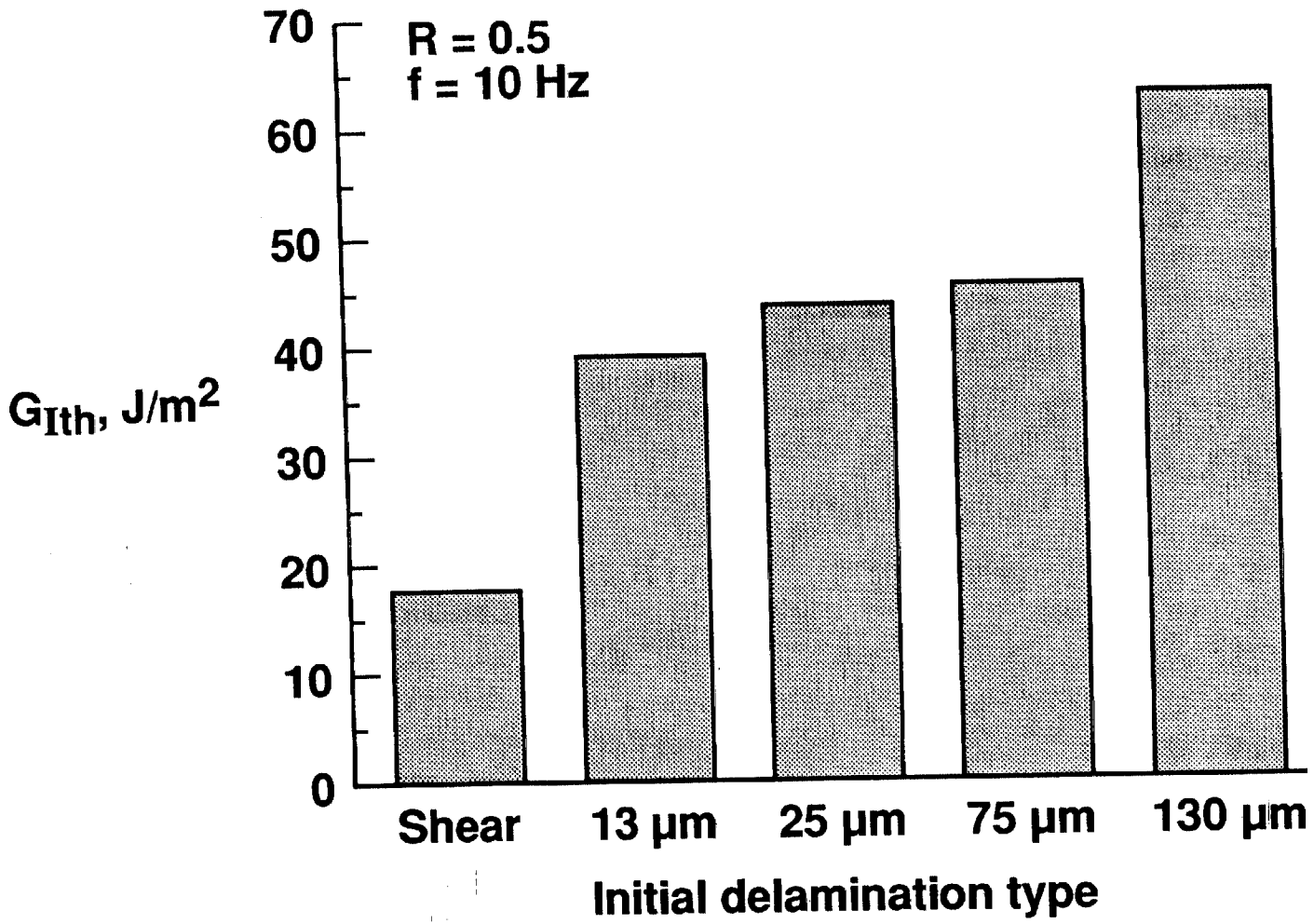

Figure 14. Effect of initial delamination on G_{Ith} in S2/SP250.

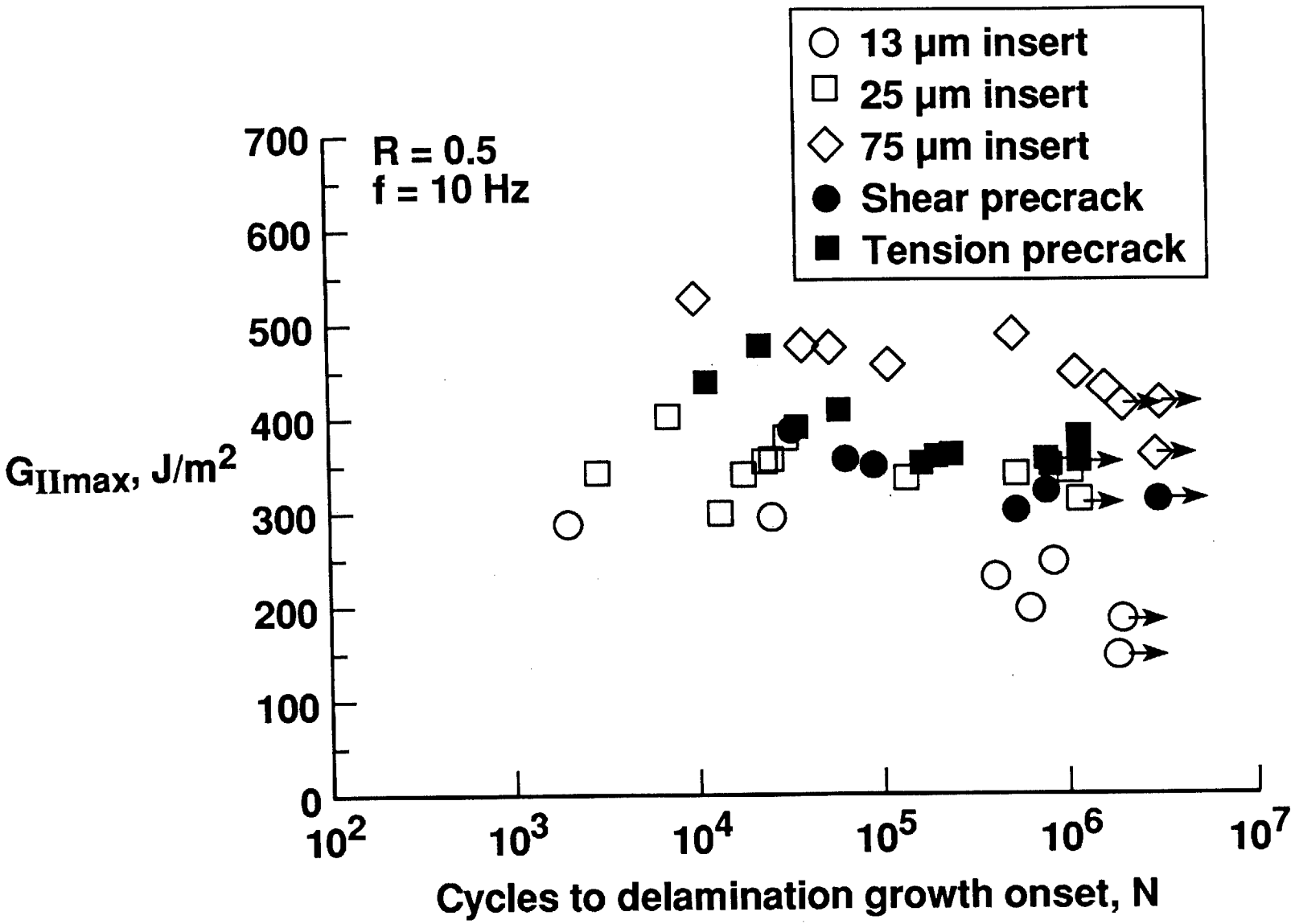

Figure 15. Fatigue delamination growth onset in S2/SP250 ENF specimens.

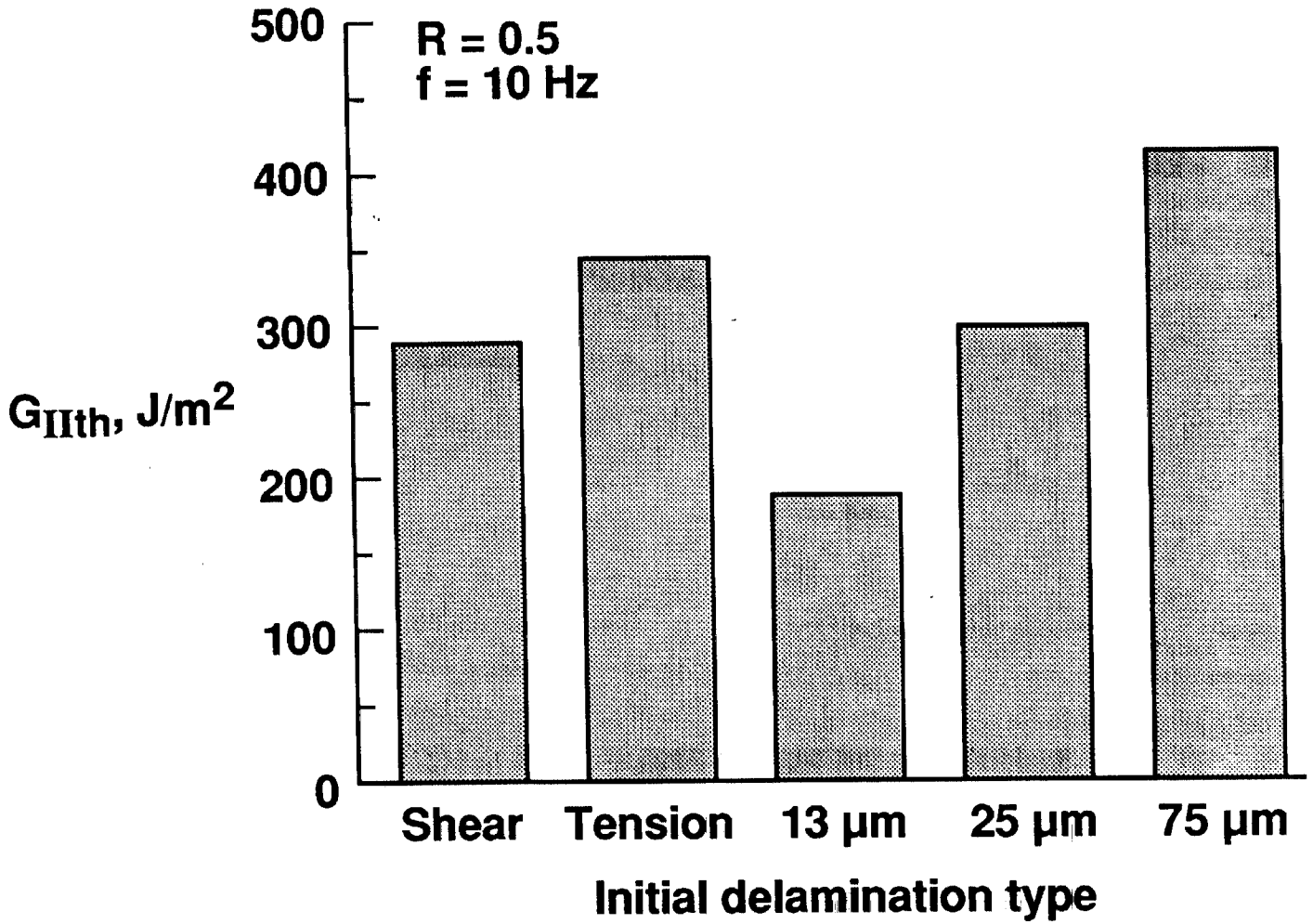

Figure 16. Effect of initial delamination on G_{IIth} in S2/SP250.

NASA National Aeronautics and Space Administration

Report Documentation Page

1. Report No.	2. Government Accession No.	3. Recipient's Catalog No.
NASA TM-104079 AVSCOM TR-91-B-005		

4. Title and Subtitle

Effect of Initial Delamination on Mode I and Mode II Interlaminar Fracture Toughness and Fatigue Fracture Threshold

5. Report Date

May 1991

6. Performing Organization Code

7. Author(s)

Gretchen B. Murri* and Roderick H. Martin**

8. Performing Organization Report No.

10. Work Unit No.

505-63-01-05

9. Performing Organization Name and Address

NASA Langley Research Center, Hampton, VA 23665-5225
U.S. Army Aviation Research and Technology Activity (AVSCOM)
Aerostructures Directorate
Hampton, VA 23665-5225

11. Contract or Grant No.

13. Type of Report and Period Covered

Technical Memorandum

12. Sponsoring Agency Name and Address

National Aeronautics and Space Administration
Washington, DC 20546-0001
U.S. Army Aviation Systems Command
St. Louis, MO 63166

14. Sponsoring Agency Code

15. Supplementary Notes

*U.S. Army Aerostructures Directorate, USAARTA-AVSCOM
**Analytical Services and Materials, Inc., Hampton, VA

16. Abstract

Static and fatigue double-cantilever beam (DCB) and end-notch flexure (ENF) tests were conducted to deter- mine the effect of the simulated initial delamination on interlaminar fracture toughness, G_c, and fatigue fracture threshold, G_{th}. Unidirectional, 24-ply specimens of S2/SP250 glass/epoxy were tested using Kapton inserts of four different thicknesses - 13, 25, 75, and 130 μm, at the midplane at one end, or with tension or shear precracks, to simulate an initial delamination. To determine G_{th}, the fatigue fracture threshold below which no delamination growth would occur in less than 1×10^6 cycles, fatigue tests were conducted by cyclically loading specimens until delamination growth was detected.

Consistent values of mode I fracture toughness, G_{Ic}, were measured from DCB specimens with inserts of thickness 75 μm or thinner, or with shear precracks. The fatigue DCB tests gave similar values of G_{Ith} for the 13, 25, and 75 μm specimens. Results for the shear precracked specimens were significantly lower than for specimens without precracks.

Results for both the static and fatigue ENF tests showed that measured G_{IIc} and G_{IIth} values decreased with decreasing insert thickness, so that no limiting thickness could be determined. Results for specimens with inserts of 75 μm or thicker were significantly higher than the results for precracked specimens or specimens with 13 or 25 μm inserts.

17. Key Words (Suggested by Author(s))	18. Distribution Statement
Delamination ENF, DCB Strain energy release rate Fracture toughness Mode I, Mode II	Unclassified - Unlimited Subject Category - 39

19. Security Classif. (of this report)	20. Security Classif. (of this page)	21. No. of pages	22. Price
Unclassified	Unclassified	39	A03